Analyst

# Disposable paper strips for carboxylate anion discrimination



| | |
|---|---|
| Journal: | *Analyst* |
| Manuscript ID | AN-ART-01-2020-000137.R1 |
| Article Type: | Paper |
| Date Submitted by the Author: | 10-Mar-2020 |
| Complete List of Authors: | Xu, Yifei; University of Alabama, Department of Chemistry and Biochemistry<br>Bonizzoni, Marco; University of Alabama, Department of Chemistry and Biochemistry; University of Alabama, Alabama Water Institute |
| | |

# Disposable paper strips for carboxylate discrimination

Yifei Xu,[a] Marco Bonizzoni*[a,b]

a. Department of Chemistry and Biochemistry, The University of Alabama, Tuscaloosa, AL, 35487 USA
b. Alabama Water Institute, The University of Alabama, Tuscaloosa, AL 35487 USA

**Abstract:** We describe a method for the differentiation of carboxylate anions on disposable paper supports (common printer paper, filter paper, chromatography paper), based on differential patterns of interactions between carboxylates and a fluorescent sensing system. The sensor was built from commercially available components, namely a polycationic fifth generation amine-terminated poly(amidoamine) dendrimer (PAMAM G5) and a small organic fluorophore (calcein) through non-covalent interactions. The assay's physical dimensions were chosen to conform to the microwell plate standard so detection could be carried out on widely available plate reader instrumentation. The sensing complex was first deposited in spots on a paper support to prepare the sensor strip; a carboxylate solution was then loaded on each spot. Nuanced changes in fluorescence were associated with carboxylate binding to the PAMAM dendrimer, characteristic of the structure and affinity of each carboxylate. Such signal changes, interpreted through Linear Discriminant Analysis (LDA), contained enough information to recognize and successfully discriminate most anions in the panel. Among the substrates we tested, chromatography paper was the most promising. The relationship between the structure of the carboxylates and the patterns giving rise to their differentiation was also discussed. Finally, the long-term stability ("shelf life") of the pre-assembled [calcein•dendrimer] sensing system was found to be excellent when deposited on paper support.

**Keywords:** carboxylate, sensing, pattern, fluorescence, dendrimer, PAMAM, noncovalent, paper

## Introduction

Selective anion recognition and sensing has been brought to the fore in supramolecular analytical chemistry due to the importance of these analytes in chemical, biological, pharmaceutical, and environmental fields.[1-5] Through non-covalent intermolecular interactions such as hydrogen bonding, hydrophobic interactions, π-π interactions,[6] guest analytes interact with a synthetic host molecule, causing changes in a measurable property typically associated with the host molecule which can be monitored to follow the binding process, e.g. through optical spectroscopy.[7, 8] Many such systems have been developed to discriminate a wide range of analytes, including metal ions,[9] amino acids,[10] nucleotides,[11] glycans,[12] bacteria,[13] odorants,[14] components

of soft drinks,[15] and wines.[16] Solution-based systems have sometimes been transitioned to solid supports,[17] in which case paper-based devices,[18-21] and sensor-soaked paper strips are particularly attractive.[22-25] Paper is a promising solid support with several advantages for sensing, such as its low cost, light weight, and long shelf life, leading to easy transportation and storage; its excellent liquid absorption characteristics, which make it a good all-purpose solid support for assays that had been developed in solution;[26] and its relative chemical inertness.[27, 28]

We became interested in carboxylate anions because of their important bioactive roles, as well as food additives, drugs, and polymer precursors or additives.[29, 30] For example, citrate has been used as an indicator in a reliable screening method for prostate cancer. In fact, normal prostatic fluid contains high levels of citrate and low levels of isocitrate; on the other hand, malignant cancer cells convert citrate to isocitrate, causing a measurable change in the citrate / isocitrate level that is diagnostically significant, leading to a need for a sensor with selectivity between the structurally similar citrate and isocitrate.[31-33] Similarly, maleate is often used in medicinal chemistry, polymer synthesis, and as a food additive, but the accumulation of maleate in the body leads to a severe kidney disease, Fanconi syndrome, so detection of maleate would also have diagnostic value.[34, 35] Additionally, most sensors for carboxylates have been developed so far to work in solution media,[36-39] a less durable and less portable alternative for in situ or point of care analysis. A simple, fast, chemoselective method to detect and differentiate common carboxylates on an inexpensive and rugged solid support such as simple paper strips can offered increased options for preliminary screening and frequent monitoring.

Our group has previously shown that the polycationic amine-terminated poly(amidoamine) (PAMAM) dendrimers can form non-covalent complexes with a variety of carboxylates,[40] as well as other anions.[41] Amine-terminated PAMAM dendrimers are globular hyperbranched polymers

that display a homogeneous array of primary amine groups on their surface, providing high capacity to bind smaller molecules in solution through non-covalent interactions.[42, 43] In this study, we used 5th generation (G5) PAMAM dendrimers (see Scheme 1), which carry 128 surface amine groups, about half of which are protonated at neutral pH, resulting in high charge density,[44] so these macromolecules can establish electrostatic and H-bonding interactions with anions, including the organic carboxylates of interest here. These polymers are also water-soluble and readily available commercially in good purity.

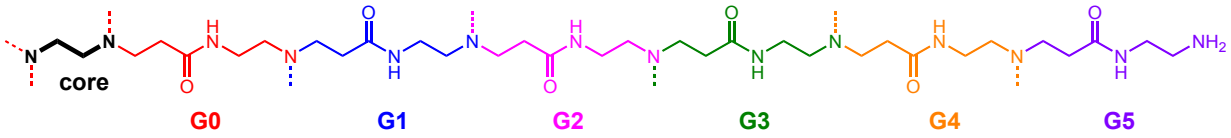


**Scheme 1.** One branch of a fifth—generation (G5) amine-terminated poly(amidoamine) (PAMAM)dendrimer with an 1,2-diaminoethane core; the dashed lines indicate the position of further branching points along the structure.

The carboxylate analytes of interest to this study are shown in Scheme 2. These structures were selected because of a combination of their biological, environmental, or industrial importance; pairs of anions with very similar structures (e.g. citrate vs. isocitrate) were also added to the panel specifically to test the extent of the discriminatory capabilities of the method discussed below.

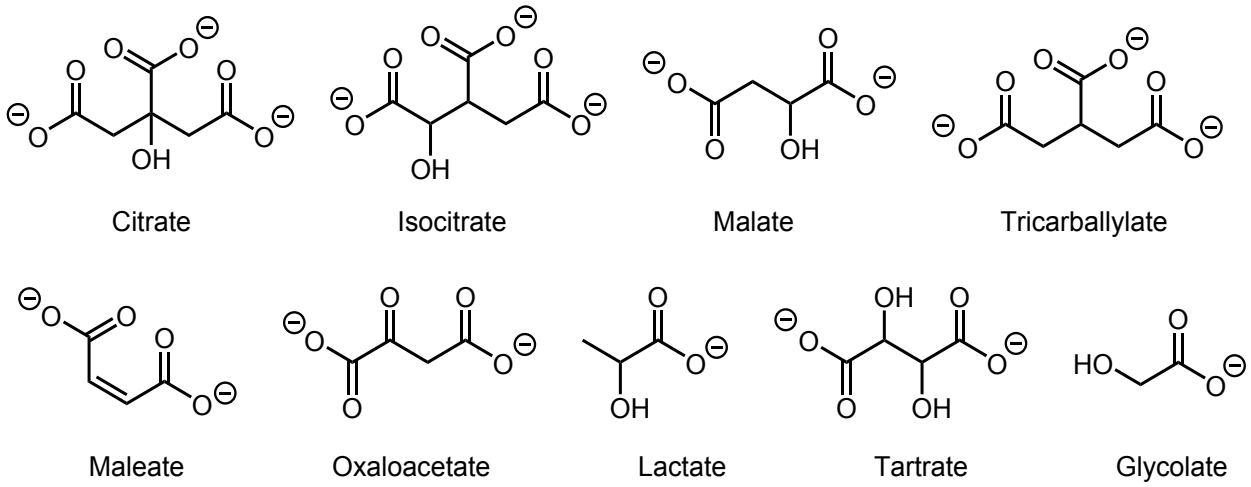


**Scheme 2.** Carboxylate anions considered in this study.

## Results and discussion

From the outset, we chose to use optical spectroscopic techniques to detect the binding and molecular recognition process, because absorbance and fluorescence measurements can be carried out rapidly and easily, and instrumentation for their measurement is very common. However, both the carboxylates and the PAMAM dendrimers are non-fluorescent and spectroscopically silent in the visible region of the spectrum, so direct observation of the interaction between these partners through optical methods was precluded to us. Instead, we endowed the dendrimer host with fluorescent properties by non-covalently bonding it to a chromogenic and fluorescent dye, giving a coloured and fluorescent [dendrimer•dye] complex that acted as a chemical sensor. This ensemble could be used in an indicator displacement assay: addition of an analyte would cause the latter to bind to the dendrimer, displacing dye molecules from the sensing complex and releasing them to the bulk. With an appropriate dye, this displacement is accompanied by a change in the optical properties of the mixture that can be used to detect the analyte binding event. In the present case, we considered 5(6)-carboxyfluorescein, calcein blue, pyranine, naphthalene-1,3,6-trisulfonate, naphthol yellow, pyrogallol red, pyrocatechol violet, glycine cresol red, alizarin red S, and calcein (see ESI Figure S1 for structures). Preliminary screening led us the selection of calcein as the dye of choice (structure in Scheme 3): calcein has good stability, is commercially available, and it is highly coloured and fluorescent; furthermore, its anionic form could bind to the cationic PAMAM dendrimer with high affinity, and yet be displaced from this complex by an excess of carboxylate analytes.

The [calcein•PAMAM] complex was first formed by adding PAMAM dendrimer to calcein dye, then the dye was displaced by addition of carboxylate. Linear Discriminant Analysis (LDA),

a pattern recognition algorithm, was used to interpret the fluorescence measurement results and discriminate the analytes. The differentiation of carboxylates has previously been studies in this group in aqueous solution on microwell plates; however, in solution this sensing complex was only stable for roughly one week. We found it necessary to develop a method that would not only work on a solid support (with the ultimate intention of developing a test strip), but also have a longer shelf life.

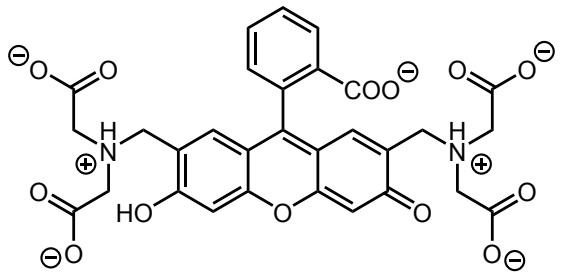


Calcein

**Scheme 3.** Chemical structure of the calcein dye.

Because we have extensive expertise in using the multiwell plate format,[41, 45-48] and because of the simplicity and ubiquity of this format in analytical as well as biological labs, we decided to take the 96-well plate format as an inspiration for the layout of our supported samples. This allowed us to use existing instrumentation (e.g. multiwell plate readers) without modification. Here we focus particularly on detection by top-detected fluorescence emission, a method which is compatible with opaque samples such as the ones discussed below.

Dye displacement assay

Spots were laid out on a solid support, using the format of a standard 96-well plates as a template, as shown below. Figure 1 demonstrates an experimental setup of a printer paper plate (the printed black rings were simply an aid to help spot the assays in the correct positions for measurement on a plate reader): Figure 1 (left) shows fresh solutions being deposited and forming

droplets on the surface of the printer paper plate; and Figure 1 (right) shows the same plate after it was allowed to dry for 2 hours. The leftmost five columns contain calcein dye samples (bright yellow); the middle five columns contain samples of [calcein•PAMAM] complex (darker orange); the last two columns contain plain HEPES buffer blanks. On printer paper plates, for instance, measurements were taken with samples both wet and dry; on the other hand, other supports (e.g. filter and chromatography paper) reliable measurements could only be obtained after the samples had dried completely. Flexible, thin paper substrates were typically taped to a rigid plastic support to reduce warping during drying.

**Figure 1.** A representative experimental set up using a paper plate: columns 1-5: calcein dye (yellow), columns 6-10: [calcein•PAMAM] complex (orange), columns 11-12: HEPES buffer blanks (clear). Left: wet droplets soon after deposition; right: samples after they were allowed to dry.

Calcein binding to PAMAM G5. We were able to ascertain that calcein binds to PAMAM dendrimers in solution (see Figure S2); we first moved to confirm that this interaction was retained on solid supports. Preliminary studies in solution were successful in carboxylate differentiation using [calcein•PAMAM] complex solutions with calcein concentration of 6.36 μM for 100 μL sample volumes. In the solid-supported experiments described below, sample volume was reduced to 1-10 μL, so we increased the initial concentration of the deposited calcein-PAMAM solutions tenfold to retain high fluorescence emission.

We first considered common chromatography paper as an inert solid support. Sample positions on these paper "plates" were chosen to coincide with the location of wells on a standard 96-well plate, so emission properties of the paper plates could be read directly in a standard multiwell plate reader, either directly depositing the paper in the reader's sample compartment, or alternatively by affixing the paper substrate with its deposited samples on a regular plastic multiwell plate to provide physical support. This approach was remarkably successful, requiring no modification to the reading routines in the multiwell plate reader; in particular, we were able to use the built-in background subtraction and automated detector gain adjustment functions directly with no issue. This greatly simplified sample measurement and allowed us significant freedom in choice of support and sample layout.

On a chromatography paper plate, we typically deposited 1 μL of a 63.6 μM solution of calcein (63.6 pmol), prepared in neutral buffered water (50 mM HEPES, pH 7.4). The solvent was allowed to evaporate; solutions containing increasing amounts of PAMAM G5 were then deposited on the calcein spots and the solvent evaporated again. The substrates were then transferred to a plate reader for measurement. As shown in Figure 2, the fluorescence emission due to calcein at 516 nm upon excitation at 485 nm decreased with increasing concentration of PAMAM G5, and reached a plateau after 21.3 picomoles of PAMAM were added. This provided evidence that the interaction of calcein with PAMAM G5 was retained on this solid support. Furthermore, we were glad to see that the fluorescence intensity of the bound calcein was reduced to 70% of that of the free dye, providing us a large dynamic range to report on the binding status of the dye. Optimization of these conditions showed us that a PAMAM G5-to-dye mole ratio of 1:3 maximized the signal dynamic range associated with the free to bound dye transition, while

still retaining high sensitivity to the addition of other analytes, so it was chosen for the studies reported below.

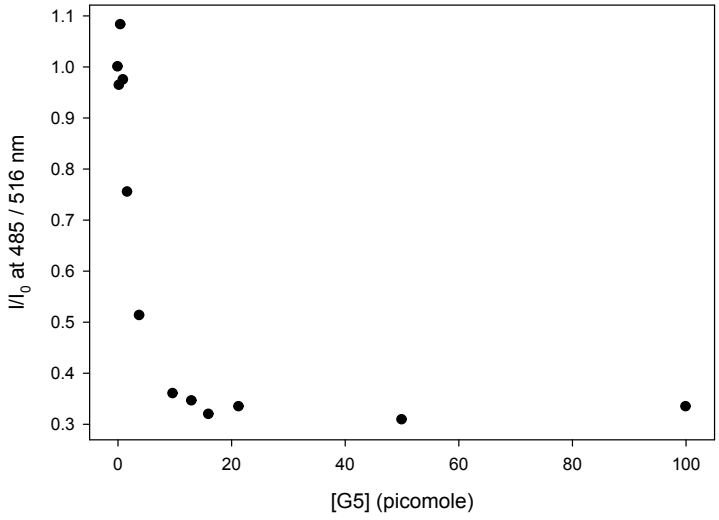


**Figure 2.** Fluorescence emission response from the calcein dye upon binding to PAMAM G5 dendrimer on chromatography paper. Excitation: 485 nm, emission: 516 nm, calcein = 63.6 pmol.

Displacement of calcein from PAMAM G5. On a chromatography paper plate, 1 μL of [calcein•PAMAM] complex solution (63.6 pmol of calcein and 21.3 pmol of PAMAM G5) was first deposited on multiple spots. After the solvent evaporated, solutions with increasing concentration of citrate anion were deposited on these "bound dye" spots. Upon addition of citrate, we expected the citrate anion, now present in large excess, to displace the calcein dye from its complex with PAMAM, resulting in a reversal of the spectroscopic trend that we had observed upon binding (Figure 2). The measured emission trend shown in Figure 3 was consistent with this hypothesis: fluorescence intensity increased and reached a maximum value similar to the emission intensity of the free calcein dye in these conditions. This indicated that the dye had been fully displaced by citrate, which in turn showed that citrate had been bound to the PAMAM dendrimer.

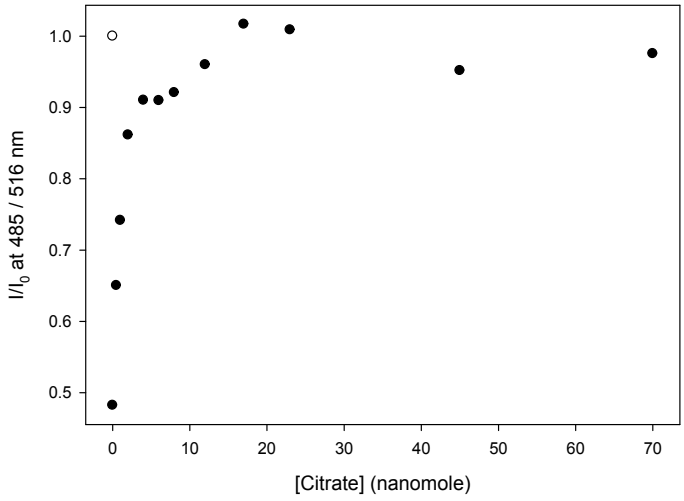


**Figure 3.** Fluorescence emission response from the calcein dye as it is displaced from its complex with PAMAM G5 by citrate on chromatography paper; the hollow dot indicates the emission of the free dye, for reference. Excitation: 485 nm, emission: 516 nm, calcein = 63.6 pmol, PAMAM G5 = 21.3 pmol.

The limit of detection (LOD) was also determined, and found to be 0.56 nanomoles (see Figure S3 in the ESI). This would be sensitive enough e.g. in medical diagnostics development (e.g. in screening for prostate cancer as described in the Introduction). The enhanced sensitivity was partly the result of the use of solid support, because even dilute solutions are pre-concentrated as a side effect of the spot drying process.

Our group's previous experience suggested that citrate, a tricarboxylate, would have a higher affinity towards the cationic PAMAM dendrimers than di- and monocarboxylates. In the following work, the [calcein•PAMAM] sensor was challenged with the same amount of each analyte. In these conditions, we expected that tricarboxylates would displace most of the dye from its complex with the dendrimer, and the fluorescence emission of the sensor system in the presence of a tricarboxylate would be similar to that of the free dye. Dicarboxylates would also lead to significant, yet incomplete displacement of the dye from its dendrimer complex: the emission of a sample containing dicarboxylate would then be similar to a mixture of free calcein and [calcein•PAMAM]

complex. Finally, monocarboxylates would only bind to the dendrimer with lower affinity and therefore displace very little of the dye, so the spectroscopic characteristics of such a sample would remain similar to the initial [calcein•PAMAM] complex. This difference in behaviour should be the main cause of differential response among tri-, di-, and monocarboxylates. This was the main contributor to the discriminatory power of this system. Furthermore, individual differences in affinity for the PAMAM dendrimer between carboxylates of the same charge contributed to a nuanced differential behaviour between these analytes, with small but significant differences that could be harnessed for the analytical discrimination of these anions.

Testing further support materials:

Transparencies and TLC plates. Transparency film (3M brand, for plain paper copiers, cellulose acetate) was first tested as an attractive support that would be inert to the aqueous solutions being used for deposition as well as transparent, and therefore may allow the use of absorbance measurements in addition to fluorescence. Because the droplets did not spread on the transparency film, these supports were found to have a high loading capacity (40 μL of solution per spot). Good fluorescence readings were obtained when the droplets were wet; however, after the droplets were allowed to dry scattering from the film's high reflectivity unfortunately overwhelmed the emission of the dye in our instrument. Although this may be obviated by modification of the reading system, this would have run counter to our goal of using unmodified instrumentation in the development of these assays, so we did not pursue this support further.

TLC plates were then tested (Merck aluminium-backed silica gel 60 plates, containing a 254 nm fluorescent indicator). Compared to transparency film, TLC plates had a much lower loading capacity (3 μL per spot); although this reduced the amount of dye present, and therefore

the analytical signal available, on the positive side this afforded much shorter drying times. This support was promising from a practical standpoint, but unfortunately further work with the TLC plates failed to retain the discriminatory power of the [calcein•PAMAM] complex (see ESI, Figure S4), so they were not pursued further.

Printer paper. Among all sources of supports we considered, printer paper (USA 11 xerographic copy paper, "92 bright", 75 g/m$^2$) is the most widely available, cheapest, and easiest to use; it also has the largest loading capacity among all paper supports (up to 10 μL per sample dot), a welcome side effect of its hydrophobic surface treatment to prevent ink bleed.[49] Like TLC plates, printer paper plates are opaque so they only allow for fluorescence measurements but, remarkably, printer paper supports allowed us to obtain measurements both when the sample spots were wet, i.e. immediately after their deposition, and after the solvent was allowed to evaporate. General-purpose office printer paper contains optical brighteners, fluorophores that typically absorb in the near UV region and emit in the blue region around 450 nm.[49] To exclude this possible source of interference, we deposited buffer spots on a paper test plate (50 mM aqueous HEPES at pH 7.4, the same medium used for all solutions) and subjected it to the same measurement conditions as the analyte plates. We found that the background emission from the paper's optical brighteners was negligible at the excitation / emission wavelength combinations used in this work, so no further correction was necessary.

Four kinds of samples, containing different carboxylates as well as calcein and PAMAM G5, were deposited on each plate. Each sample was replicated 9-fold on each plate; 12 fluorescence emission measurements were taken using a standard microwell plate reader and different combinations of excitation and emission wavelengths. Measurements were taken right after

deposition, when the samples were wet, and after 2 hours, when the solvent had evaporated and the spots were dry. Each sample on the plate was thus associated with 12 fluorescence measurement results, at various combinations of excitation and emission wavelengths, generating a 12-dimensional dataset. This dataset was subjected to Linear Discriminant Analysis (LDA) to extract the information most useful for anion discrimination, followed by manual dimensionality reduction on the basis of the LDA results. LDA transforms the original dataset into a new one of the same dimensionality, generated by linear combinations of the original one; the LDA algorithm determines appropriate weights to use in the linear combination that guarantee that each new descriptor contains as much information as can be "crammed into it" by linear combination of the original instrumental measurements; results of LDA analysis are also listed in order of decreasing information content. Samples can then be described by their coordinates along these new descriptors; these new coordinates are typically referred to as "factor scores" in the context of LDA analysis. This analysis also provides information about the information content of the original descriptors (i.e. the raw instrumental measurements), typically presented as a "loadings plot" (see e.g. Figure S8). Inspection of the loadings plot obtained from LDA analysis hints at the chemical sources of the discriminatory power in the sensing system at hand. This allowed us to interpret the observed differences among anions in light of their chemical structure and properties, as outlined in the discussion below. Finally, the dimensionality of the data set was reduced by retaining only the first two descriptors obtained from LDA and discarding the rest; we were able to retain most of the information present in the original raw data set, while at the same time drastically reducing its complexity, and allowing us to present the results in a simple two-dimensional scatter plot (typically referred to as a "score plot").

As a proof of principle, we first attempted the differentiation of four representative carboxylates from the analyte panel shown in Scheme 2 using the [calcein•PAMAM] sensor on printer paper supports, namely citrate and isocitrate, maleate, and oxaloacetate. The combined measurements obtained from both wet and dry spots were analyzed by LDA as mentioned above; the results are shown as a scores plot in Figure 4a. Here factor 1 accounts for 60.3% of the original information while factor 2 contains 27.2%, so 87.5% of the original information was retained after data reduction, an excellent result. Each carboxylate sample was replicated 8 times on the plate. The separation results feature tight clusters of replicates, indicating good repeatability of the deposition and measurement processes; and large inter-cluster separations, an indication of the strong discriminatory power of the [calcein•PAMAM] sensing complex towards these carboxylates on the printer paper support. It was particularly noteworthy that citrate and isocitrate, very similar by chemical structure and typically difficult to separate, were also clearly differentiated. This was a very encouraging first result which led us to continue consideration of printer paper as a solid support for our application.

The results above were obtained by depositing the sensor and analyte on the solid support at the same time; in practice, however, one would expect to use this system as a "test strip" of sorts, preloaded with sensor and ready to accept the analyte solution. We therefore first deposited the sensing complex on the paper support and let these spots dry completely; carboxylates were then deposited on these dry spots in a separate step. Measurements were taken on both the wet and dry spots, as done previously; after LDA analysis, the results are reported in Figure 4b. Once more, all carboxylates were differentiated successfully, indicating that the pre-deposited [PAMAM G5-calcein] complex still retains its discriminatory power in these conditions, and it bodes well for the development of a practical paper-based sensing strip based on this system.

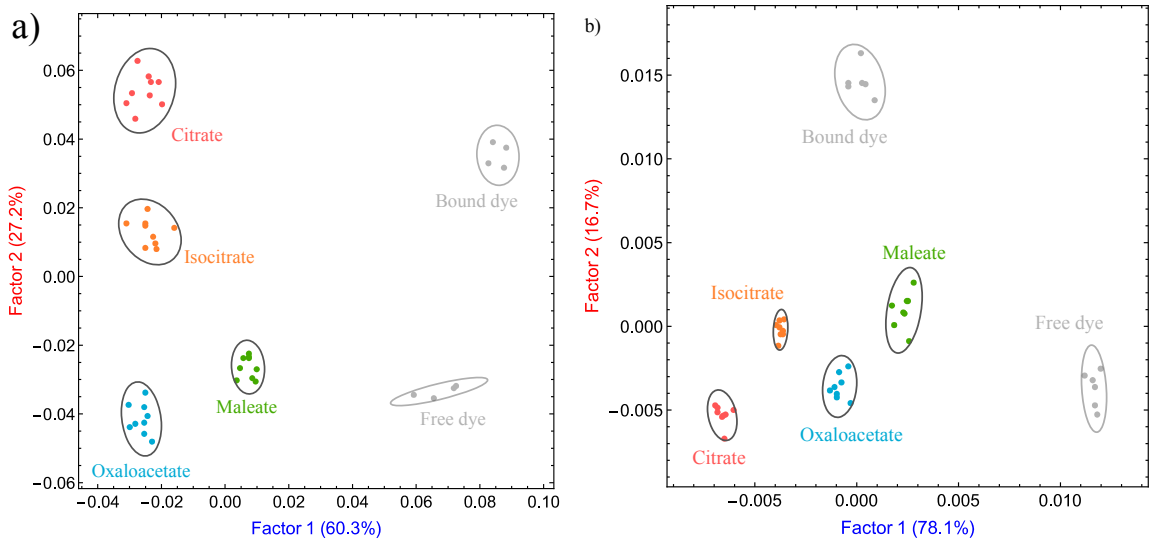


**Figure 4.** LDA scores plots obtained for the differentiation of citrate, isocitrate, maleate, and oxaloacetate on printer paper as solid support. a) In this case, the [calcein•PAMAM] complex and the carboxylate analytes were deposited together; b) In this case, the sensing complex was deposited on the paper support first, the solvent allowed to evaporate, and then the carboxylate analytes were added in a second step.

Although we obtained encouraging results using plain printer paper as solid support for our assay, there were still some significant disadvantages: for one, the results were very sensitive to the correct positioning of the droplets when measured wet; the separation between sample spots also had to be relatively large to reduce cross-talk (for this reason, we used every other "well" on our printer paper plates, although this reduced sample density and throughput); the paper support warped during drying, so we had to secure it to a rigid plastic support when carrying out the measurements (for convenience, we used a plastic 96-well plate, since it was easily available and it naturally fit in the instrument's sample holder). Deposited spots also took a disappointingly long time to dry completely on this support (2 hr), which significantly slowed the measurement process. We attempted to base the differentiation only on the measurements obtained while the sample spots were still wet, but the discrimination results were poor (see ESI, Figure S5a). The dry-spot measurements alone gave better results (see ESI, Figure S5b), but the analytes were still not fully differentiated. Good differentiation was only obtained when combining the measurements

obtained with wet and dry sample spots, but this made the process inherently slow and cumbersome, so we decided to seek a better support and moved on to filter paper.

Filter paper. We used Whatman 597, diameter 150 mm filter paper circles. Fluorescence measurements can easily be taken on this support, which is also sturdier than office paper and less prone to deformation when wet. Although filter paper has higher absorbing capacity than office paper, our initial attempts at higher loading generated wide, poorly defined sample spots and high sample crosstalk, so spot loading had to be reduced to 1 μL on this support; on the plus side, this significantly reduced drying times. According to the successful "test strip" protocol developed above, the [calcein•PAMAM] sensing complex was first deposited on the paper and allowed to dry, then five different carboxylate solutions were deposited, each replicated 16-fold. The plate was read after solvent evaporation; data reduction and interpretation were performed using Linear Discriminant Analysis (LDA) as discussed previously. The results are shown in Figure 5 as an LDA score plot. Using this support, we obtained overall better differentiation than with printer paper plates, with no overlapping clusters, even though the amount of sensor and analytes was much lower than before, due to the low spot loading. However, the discriminatory power of the system on this support was similar, as evidenced by the relatively large fact that the size of the replicate clusters was sometimes comparable to the inter-cluster distance, i.e. to the separation between different analytes. Therefore, we sought to further improve the method by exploring a similar support.

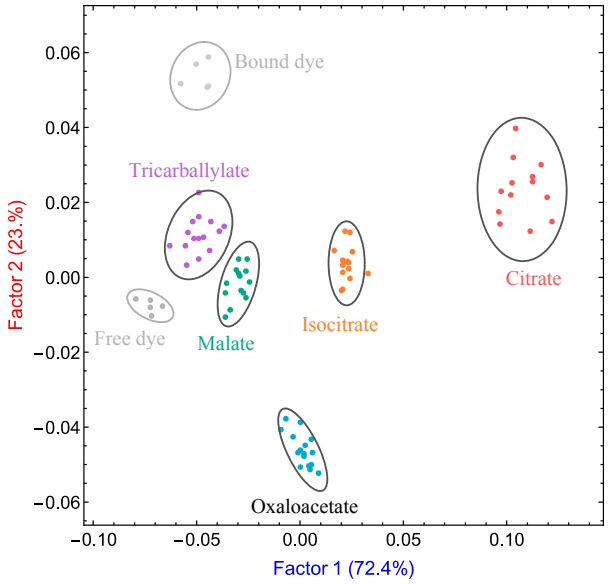


**Figure 5.** LDA scores plot for the differentiation of citrate, isocitrate, malate, oxaloacetate, and tricarballylate on filter paper plates.

Chromatography paper. Chromatography paper (Whatman Chromatography paper, 1CHR) was very similar to the previously used filter paper, although thicker. The loading capacity of chromatography paper plates increased to 2.5 µL. The same set of five analytes used on filter paper supports (citrate, isocitrate, malate, tricarballylate, and oxaloacetate, see Figure 5 above) was first tested on chromatography paper, in the same conditions. 2.5 µL of a solution of [calcein•PAMAM] complex (63.6 µM in calcein and 21.3 µM in PAMAM G5, = 159 pmol of calcein and 53.25 pmol of PAMAM G5) were loaded on the chromatography paper support, followed by 2.5 µL of a 0.023 M solution of carboxylates (57.5 nmol) after the sensor spots had dried. The data acquisition and interpretation were carried out as described before. Results are shown in Figure 6a: smaller, tighter replicate clusters showed that chromatography paper plates enable a higher discriminatory power; the contribution of each factor is more even, indicating that multiple independent instrumental measurements were contributing. Among all carboxylates, the citrate cluster was

found far from the rest of the other anions on the scores plots, possibly due to the formation of a [calcein-PAMAM-citrate] three-body complex, not apparent in the other analytes.

Chromatography paper supports were also compared directly to printer paper ones, the first support we considered; their performance was much higher in that case as well (see ESI, Figure S6). Finally, the use of chromatography paper supports also led to improved repeatability, as shown in Figure 6b: combining data from two replicates of the same plate, separately prepared, led to repeatable results and no degradation of the discriminatory power. The chromatography paper's higher loading capacity vs. other paper supports was likely the main contributor to improved performance: the thicker, more robust support allowed us to use more material in each spot with minimal warping and easier handling.

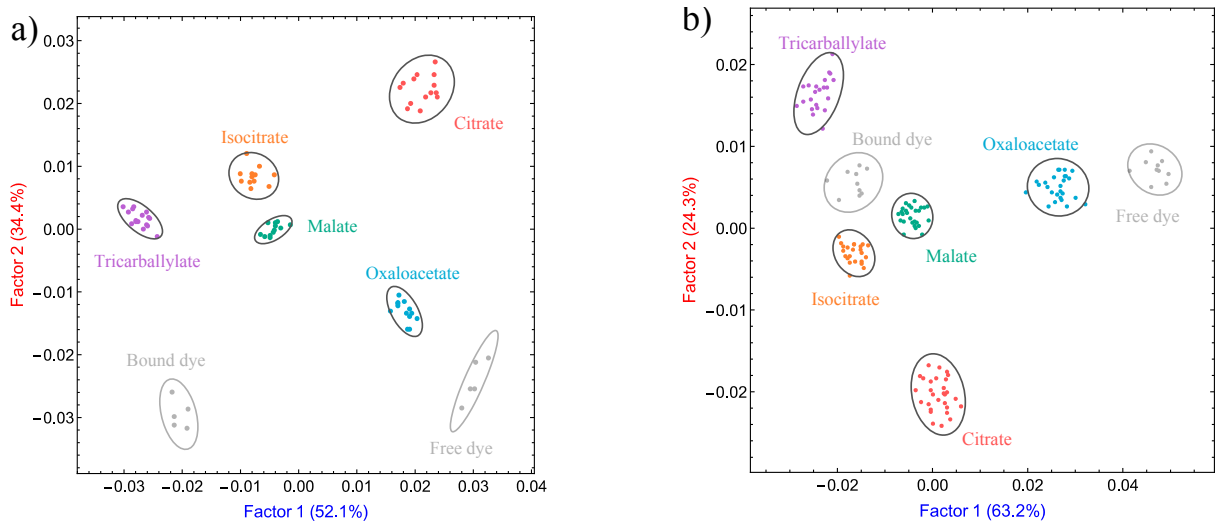


**Figure 6.** LDA scores plot for the differentiation of citrate, isocitrate, oxaloacetate, malate, tricarballylate on chromatography paper plates. Left, a) Scores plot from a single plate; Right, b) The scores plot obtained by combining data from two separate plates with identical contents shows comparable results, confirming excellent repeatability.

Our group's previous work has shown that PAMAM dendrimers behave as hydrogen bond acceptors,[40] so they are often sensitive to the presence of hydroxy groups on their binding partners.[45] We endeavoured to test whether this effect was still active on solid support. We therefore selected common carboxylates containing hydroxy groups as analytes and attempted

their discrimination on chromatography paper. The results in Figure 7 show that most of the carboxylates were differentiated. In the scores plot, replicate clusters corresponding to monocarboxylates lactate and glycolate appear very close to the "bound dye" cluster, i.e. the [calcein•PAMAM] complex, whereas dicarboxylates oxaloacetate, malate, and tartrate generate clusters close to the calcein free dye. Since attractive electrostatic interactions provide much of the driving force for carboxylate binding, dicarboxylates have higher affinity towards dendrimer than monocarboxylates, so in our system a dicarboxylate would displace the dye more completely from its dendrimer complex than an equal amount of a monocarboxylate, and such a sample would mostly contain free dye, therefore being spectroscopically similar to a dye reference sample. Oxaloacetate, a dicarboxylate containing an OH group thanks to its prominent enol form, seemed to display the highest affinity, as indicated by the position of its cluster, very close to the free dye's. Proximity to the "free dye" cluster indicates that, in samples containing oxaloacetate, most of the dye had been displaced from its complex with the dendrimer, therefore appearing free. On the other hand, monocarboxylates have lower affinity to the dendrimer and their binding is less complete, therefore these samples are spectroscopically very similar to the "bound dye" [calcein•PAMAM] complex (and to each other!), reducing the discriminatory power of the system towards these analytes. Furthermore, the two tricarboxylates in the panel, citrate and isocitrate, are spectroscopically clearly distinct from either the sensing complex ("bound dye") or the free dye reference, possibly because of the formation of a three-component [anion-PAMAM-dye] complex with radically different spectroscopic properties. Finally, the malate and tartrate sample clusters fall very close to each other, although tartrate has one more hydroxyl group than malate. This indicated to us that the affinity enhancement favouring hydroxy-containing substrates is less

effective in these solid supported media. In the absence of solvent, the carbohydrate units in the paper itself might interfere with these processes, saturating the dendrimer's ability to accept hydrogen bonds.

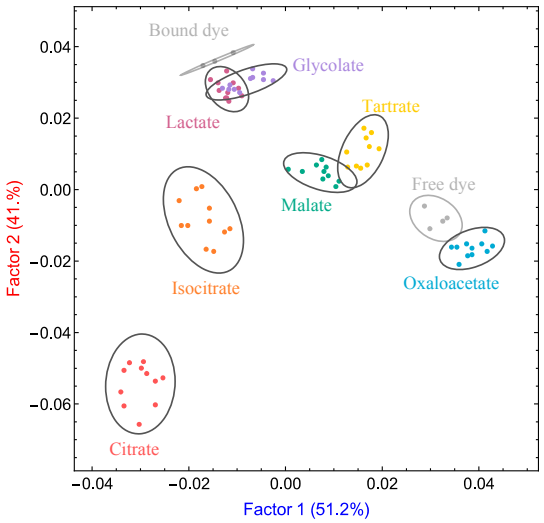


**Figure 7.** LDA scores plot for the differentiation of citrate, isocitrate, oxaloacetate, malate, tartrate, lactate, and glycolate using the [calcein•G5 PAMAM] sensor deposited on chromatography paper. Reference samples for the free and dendrimer-bound calcein dye are also included, as "free dye" and "bound dye" respectively.

We also re-analysed the measurements from the experiment just described by excluding the data corresponding to the free and fully bound dye (these are typically included on the plates as reference samples, to check inter-plate consistency and for detector calibration). Being often substantially different from any of the carboxylate samples, these samples may skew the analysis, being given excessive weight by the LDA algorithm. This had been the case on other solid supports; consider, for instance, our attempt to use printer paper described before (see Figure 4a), in which differences along factor 1 overwhelmingly reported on the difference between the bound and free dye reference clusters and all the other carboxylate analytes. To accentuate the differences among the analytes, we re-ran the LDA analysis excluding data from the free and bound dye reference samples. The LDA scores plot resulting from this analysis is shown in Figure 8a (the corresponding loading plot is shown in Figure S8). We were pleased to see that the relative positions of the analyte

clusters were similar, indicating that the system captures intrinsic underlying chemical similarities and differences between these analytes, while slightly increasing the distances between analyte clusters, as desired.

Finally, Figure 8b shows the results of measurements of three identical replicate plates: the positions of the analyte clusters are very similar to those obtained from a single plate (Figure 8a), proving the excellent repeatability of this method.

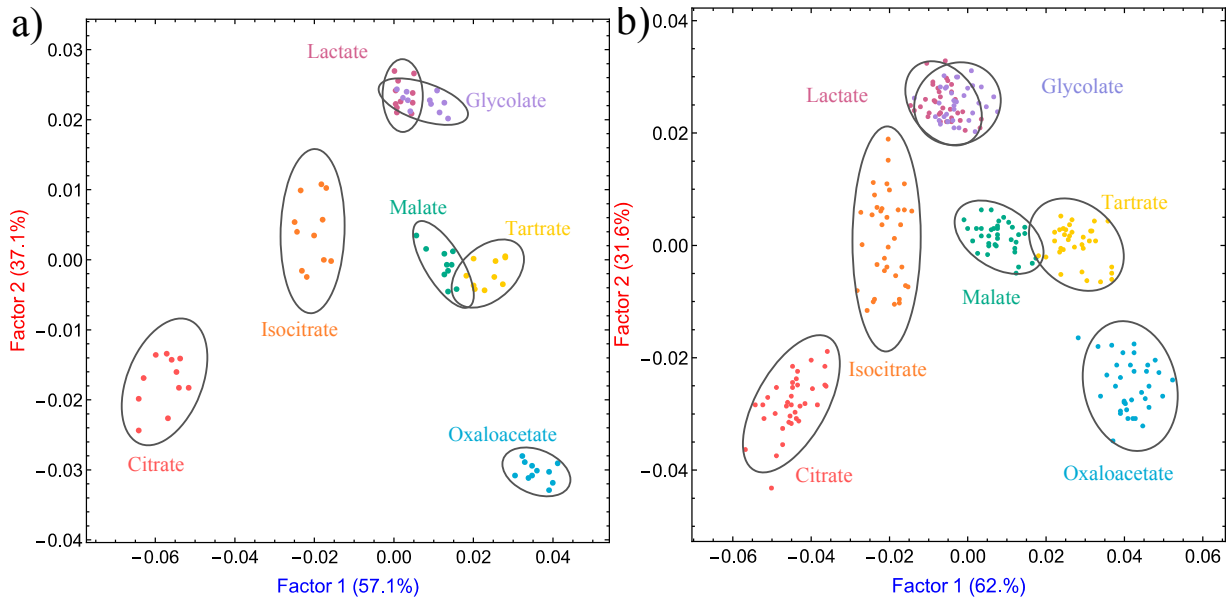


**Figure 8.** LDA scores plot of for the differentiation of the same group of anions on chromatography paper. From left: a) scores plot for the same plate shown in Figure 7 above, from which the reference samples have been removed; b) scores plot obtained from combining data from three separately prepared replicates of the same plate, to showcase the repeatability of this technique.

## Cost analysis

A cost comparison with solution-based systems (Table S2 in the ESI) was made between the use of a 96-well black wall polystyrene plate (as commonly used for fluorescence studies), and the most promising solid supports shown here (printer paper, filter paper, and chromatography paper). Including the price of the support material as well as the sensor complex, screening 96 samples on the plastic plate in solution would cost $3-$4; the same experiment carried out on

printer paper, filter paper, and chromatography paper was estimated to lead to at least tenfold cost reduction (namely, $0.01, $0.25, and $0.30, respectively), the differences in cost being mainly due to the price of the support material and the reduced polymer consumption.

Shelf life of sensor-loaded plates

As mentioned in the introduction, the [calcein•PAMAM] complex is only stable for about a week when stored as a solution in aqueous buffer; this is likely due to dye decomposition, since in our hands the G5 PAMAM dendrimer component is stable indefinitely in that medium. Therefore, we were interested in testing the stability of the [calcein•PAMAM] complex and of the free dye on our most promising solid support, chromatography paper, after solvent removal. We hoped to observe increased stability of the pre-formed [calcein•PAMAM] complex in the solid state, which would allow us to develop ready-to-use sensing plates with pre-deposited sensing complex and reference spots.

Long-term stability ("shelf life") experiments were performed on three chromatography paper plates. Each plate contained 20 replicates of a free dye sample, and 20 replicates of a [calcein•PAMAM] complex sample, deposited under the same conditions described in the work above. Fluorescence emission measurements for these plates were recorded over 33 days. Between measurements, the paper plates were stored in sealed polyethylene bags, away from light. The results are shown in Figure 9 as a function of time; each bar was obtained as the average of 60 replicates from the three separate but identical plates (20 replicates of each sample type per plate, over a total of 3 plates). In the first 18 days, the fluorescence emission intensity remained remarkably constant; marked decreases were only observed around day 19, slowly losing intensity thereafter. Compared with solution behaviour, deposition on this solid support was shown to

increase the dye's and complex's stability at least twofold, a promising result for further practical development.

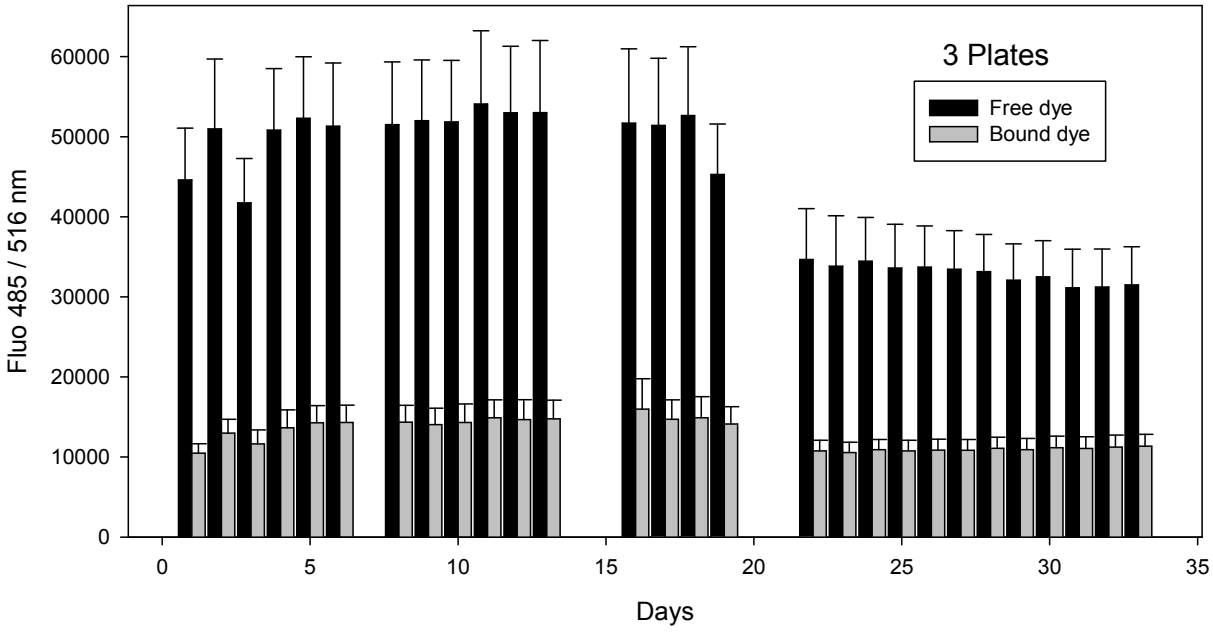


**Figure 9.** The stability of free dye and [calcein•PAMAM] samples was monitored using fluorescence emission measurements after deposition on chromatography paper plates; calcein = 63.6 pmol, PAMAM G5 = 21.3 pmol; excitation: 485 nm, emission: 516 nm; spots were laid out on each plate as shown in **Figure 1**. Each bar is an average of 60 replicates across three different plates; corresponding error bars (95% confidence) are provided as well.

## Conclusions

This study shows that the binding of the anionic calcein dye to the PAMAM dendrimer polycation and its displacement are active on a variety of solid supports and can be monitored using fluorescence measurements carried out using common formats and standard instrumentation. Different support media were studied, including cellulose acetate transparency film, silica TLC plates, common office printer paper, filter paper, and chromatography paper. All cheaper than common polystyrene 96-well plates, they also have the advantage of requiring less sensor material, as well as needing less analyte than the same measurement carried out on microwell plates. Among all supports, common printer paper was the cheapest and most widely available, but the system

showed low analytical discrimination ability on this support. Filter paper afforded better differentiation than printer paper, using even less material, due to lower loading capacity. Finally, the sturdier chromatography paper was found to perform the best, with excellent analytical differentiation results even at low loading. We also found it to afford excellent repeatability and improved shelf life for the dye and sensing complex when compared to the same system in solution. Overall, this affordable and easy to use support offers promising opportunities for further development of inexpensive disposable solid-supported chemical sensing systems.

## Experimental

Materials. Poly(amidoamine) (PAMAM) Generation 5 (G5) dendrimers were purchased from Dendritech, Inc., as 5.01 wt.% methanol solution with density of 0.802 g/mL at 23°C. The solutions used in this study contained a negligible amount of methanol (<0.8%) after dilution from this stock. Calcein dye was purchased from Sigma Aldrich and was used as received. DL-malic acid and oxaloacetic acid were purchased from Sigma Aldrich; maleic acid, tricarballylic acid, and sodium L-lactate from Alfa Aesar; DL-isocitric acid trisodium salt hydrate and sodium glycolate from ACROS Organics; anhydrous citric acid from EMD Millipore; and potassium sodium (+)-tartrate tetrahydrate from TCI. All carboxylic acids / carboxylates were used as received. All solutions were prepared in 50 mM 4-(2-hydroxyethyl) piperazine-1-ethanesulfonic acid (HEPES) buffer (purchased from IBI Scientific) dissolved in DI water and adjusted to pH 7.4. When necessary, pH adjustments were carried out by the addition of NaOH (Fisher Scientific) or HCl (BDH) solutions. Nunc 96-well polystyrene plates were purchased from Thermo Scientific. Silica gel 60 aluminum-backed TLC sheets were purchased from EMD Millipore. Chromatography paper (1 CHR) and filter paper (150 mm diameter circles) were purchased from Whatman. Office xerographic printer paper (US Letter size, 92 brightness, 75 g/m$^2$) was obtained from Staples.

Instrumentation. Sample spots were printed or drawn on solid supports as shown in Figure 1. Sample solutions were deposited by hand using Eppendorf Research multichannel pipettors with VWR brand disposable plastic tips. A Biotek Synergy II multimode microwell plate reader was used for the collection of fluorescence emission intensities, through bandpass filters. 12 combinations of excitation/emission wavelengths were measured for each sample ($\lambda_{ex}/\lambda_{em}$): 450/516 nm, 450/528 nm, 450/560 nm, 450/580 nm, 460/516 nm, 460/528 nm, 460/560 nm, 460/580 nm, 485/516 nm, 485/528 nm, 485/560 nm, 485/580 nm.

Experimental conditions. Total solution volume for each spot was determined to be the maximum amount that would not spread outside of the designated spot area during the deposition and drying process, and the maximum amount that would not lead to dye self-quenching after drying. An optical deposited amount was determined for each solid support and used for all experiments on that support: 40 μL per spot for transparencies; 3.0 μL per spot for TLC plates; 10 μL per spot for printer paper; 1.0 μL per spot for filter paper; 2.5 μL per spot for chromatography paper.

Solid-supported experiments. Stock solutions of calcein and dendrimers in buffer were used as starting points, and carboxylate solutions were made fresh every time. Binding of calcein to PAMAM: For binding experiment, 1.0 μL of 63.6 μM calcein solution (63.6 pmol) was deposited on each designated spot and allowed to dry. 1.0 μL of solutions containing increasing concentration of PAMAM G5 dendrimer was then deposited on the dried calcein spots. Fluorescence emission was measured. Binding of citrate, detected by indicator displacement: An optimal molar ratio of calcein and dendrimer to form the [calcein•PAMAM] complex was determined to be 3:1; based on our group's previous experience, these conditions optimize the sensitivity and responsiveness of an indicator displacement assay. On a new plate, a mixture of

calcein and G5 PAMAM containing this ratio was spotted on the support, followed by 1.0 μL of citrate solutions of increasing concentrations. Each titration was carried out in 7 replicates; fluorescence intensity measurements (excitation at 485 nm; emission at 516 nm) were collected in a Biotek Synergy II microwell plate reader. Carboxylate differentiation experiments: For differentiation experiments, depending on the number of analytes, 9 to 16 replicates were laid out for each analyte. The fluorescence emission of the samples was read directly on the solid support using the microwell plate reader configured for reading a standard 96-well plate; the fluorescence detector gain was adjusted so that the strongest fluorescence emission on each plate reached 85% of the instrument's full scale. Aqueous HEPES buffer (50 mM, pH 7.40) was used as a blank.

Data processing. Data acquired from the plate reader included 12 fluorescence emission measurements as the 12 variables for the experiment. Wolfram Research's *Mathematica* v. 12 was used for data processing, using routines developed in-house for LDA analysis and data presentation. Upon inspection of the raw data, measurements from those excitation / emission channels for which little signal was present from the calcein dye and were therefore exceedingly noisy were dropped from the dataset. Then, outlier tests were performed among the replicates of each analyte: any replicate that was found outside a 95% confidence interval around the multivariate mean for each cluster was removed from the dataset (see ESI, Figure S7). 12 variables were then transformed to 12 factors using the Linear Discriminant Analysis (LDA) algorithm, the first two factors were retained, and scores along those two factors were used to build 2D scatterplots (LDA "scores plots") as shown in the results above.

**Conflicts of interest**

There are no conflicts to declare.

**Acknowledgements**

The authors gratefully acknowledge support from the Alabama Water Institute (AWI) at The University of Alabama, and funding from the US National Science Foundation (OIA 1632825).

## References


1. P. Anzenbacher, Jr., P. Lubal, P. Bucek, M. A. Palacios and M. E. Kozelkova, *Chem. Soc. Rev.*, 2010, **39**, 3954-3979.
2. G. W. Bates and P. A. Gale, *Struct. Bonding (Berlin, Ger.)*, 2008, **129**, 1-44.
3. P. Karmakar, S. Manna, S. S. Ali, U. N. Guria, R. Sarkar, P. Datta, D. Mandal and A. K. Mahapatra, *New J. Chem.*, 2018, **42**, 76-84.
4. A. Brugnara, F. Topic, K. Rissanen, A. de la Lande, B. Colasson and O. Reinaud, *Chem. Sci.*, 2014, **5**, 3897-3904.
5. A. Schaly, R. Belda, E. Garcia-Espana and S. Kubik, *Org. Lett.*, 2013, **15**, 6238-6241.
6. J. K. M. Sanders, *Angew. Chem., Int. Ed. Engl.*, 1995, **34**, 2563.
7. L. You, D. Zha and E. V. Anslyn, *Chem. Rev. (Washington, DC, U. S.)*, 2015, **115**, 7840-7892.
8. M. I. J. Stich, L. H. Fischer and O. S. Wolfbeis, *Chem. Soc. Rev.*, 2010, **39**, 3102-3114.
9. S. S. Tan, S.-J. Kim and E. T. Kool, *J. Am. Chem. Soc.*, 2011, **133**, 2664-2671.
10. A. Buryak and K. Severin, *J. Am. Chem. Soc.*, 2005, **127**, 3700-3701.
11. J. Gao, A. Granzhan, X. Qian and K. Severin, *Chem. Commun. (Cambridge, U. K.)*, 2010, **46**, 5515-5517.
12. K. L. Bicker, J. Sun, M. Harrell, Y. Zhang, M. M. Pena, P. R. Thompson and J. J. Lavigne, *Chem. Sci.*, 2012, **3**, 1147-1156.
13. R. L. Phillips, O. R. Miranda, C.-C. You, V. M. Rotello and U. H. F. Bunz, *Angew. Chem., Int. Ed.*, 2008, **47**, 2590-2594.
14. T. Takeuchi, J. Montenegro, A. Hennig and S. Matile, *Chem. Sci.*, 2011, **2**, 303-307.
15. C. Zhang and K. S. Suslick, *J. Agric. Food Chem.*, 2007, **55**, 237-242.
16. A. P. Umali, S. E. LeBoeuf, R. W. Newberry, S. Kim, L. Tran, W. A. Rome, T. Tian, D. Taing, J. Hong, M. Kwan, H. Heymann and E. V. Anslyn, *Chem. Sci.*, 2011, **2**, 439-445.
17. A. Akdeniz, M. G. Caglayan and P. Anzenbacher, *Chem. Commun.*, 2016, **52**, 1827-1830.
18. A. K. Ellerbee, S. T. Phillips, A. C. Siegel, K. A. Mirica, A. W. Martinez, P. Striehl, N. Jain, M. Prentiss and G. M. Whitesides, *Anal. Chem. (Washington, DC, U. S.)*, 2009, **81**, 8447-8452.
19. J. G. Bell, M. P. S. Mousavi, M. K. Abd El-Rahman, E. K. W. Tan, S. Homer-Vanniasinkam and G. M. Whitesides, *Biosens. Bioelectron.*, 2019, **126**, 115-121.
20. Q.-M. Feng, M. Cai, C.-G. Shi, N. Bao and H.-Y. Gu, *Sens. Actuators, B*, 2015, **209**, 870-876.
21. Q. Wang, X. Li, L. Tang, Y. Fei, Y. Pan and L. Sun, *J. Appl. Phycol.*, 2019, Ahead of Print.
22. D. K. Das, S. Deka and A. K. Guha, *J. Fluoresc.*, 2019, **29**, 1467-1474.
23. P. Jaikang, P. Paengnakorn and K. Grudpan, *Microchem. J.*, 2020, **152**, 104283.
24. M. Jaeger, S. Schubert, S. Ochrimenko, D. Fischer and U. S. Schubert, *Chem. Soc. Rev.*, 2012, **41**, 4755-4767.
25. Y. Kim, G. Jang and T. S. Lee, *ACS Appl. Mater. Interfaces*, 2015, **7**, 15649-15657.
26. E. J. Maxwell, A. D. Mazzeo and G. M. Whitesides, *MRS Bull.*, 2013, **38**, 309-314.
27. E. W. Rice, *J. Ind. Eng. Chem. (Washington, D. C.)*, 1912, **4**, 229.
28. G. S. Walpole, *Biochem J*, 1913, **7**, 260-267.
29. S.-Y. Liu, L. Fang, Y.-B. He, W.-H. Chan, K.-T. Yeung, Y.-K. Cheng and R.-H. Yang, *Org. Lett.*, 2005, **7**, 5825-5828.
30. A. Metzger and E. V. Anslyn, *Angew. Chem., Int. Ed.*, 1998, **37**, 649-652.
31. , BR2011003546A2, 2014.
32. K. M. Selnaes, I. S. Gribbestad, H. Bertilsson, A. Wright, A. Angelsen, A. Heerschap and M.-B. Tessem, *NMR Biomed.*, 2013, **26**, 600-606.
33. L. C. Costello and R. B. Franklin, *Prostate Cancer Prostatic Dis*, 2009, **12**, 17-24.

34. E.-J. Kim, U. Haldar and H.-i. Lee, *Polymer*, 2019, Ahead of Print.
35. S. Eiam-Ong, M. Spohn, N. A. Kurtzman and S. Sabatini, *Kidney Int.*, 1995, **48**, 1542-1548.
36. K. Ghosh and I. Saha, *Tetrahedron Lett.*, 2008, **49**, 4591-4595.
37. Z.-h. Chen, Y.-b. He, C.-G. Hu and X.-h. Huang, *Tetrahedron: Asymmetry*, 2008, **19**, 2051-2057.
38. D.-S. Kim and K. H. Ahn, *J. Org. Chem.*, 2008, **73**, 6831-6834.
39. A. Sheini, H. Khajehsharifi, M. Shahbazy and M. Kompany-Zareh, *Sens. Actuators, B*, 2017, **242**, 288-298.
40. A. M. Jolly and M. Bonizzoni, *Macromolecules (Washington, DC, U. S.)*, 2014, **47**, 6281-6288.
41. X. Liang and M. Bonizzoni, *J. Mater. Chem. B*, 2016, **4**, 3094-3103.
42. D. A. Tomalia, H. Baker, J. Dewald, M. Hall, G. Kallos, S. Martin, J. Roeck, J. Ryder and P. Smith, *Polym. J. (Tokyo, Jpn.)*, 2002, **34**, 132-147.
43. M. Tang, C. T. Redemann and F. C. Szoka, Jr., *Bioconjugate Chem.*, 1996, **7**, 703-714.
44. Y. Niu, L. Sun and R. M. Crooks, *Macromolecules*, 2003, **36**, 5725-5731.
45. A. M. Mallet, Y. Liu and M. Bonizzoni, *Chem. Commun. (Cambridge, U. K.)*, 2014, **50**, 5003-5006.
46. A. M. Mallet, A. B. Davis, D. R. Davis, J. Panella, K. J. Wallace and M. Bonizzoni, *Chem. Commun. (Cambridge, U. K.)*, 2015, **51**, 16948-16951.
47. Y. Liu and M. Bonizzoni, *J. Am. Chem. Soc.*, 2014, **136**, 14223-14229.
48. X. Liang, M. Trentle, V. Kozlovskaya, E. Kharlampieva and M. Bonizzoni, *ACS Appl. Polym. Mater.*, 2019, **1**, 1341-1349.
49. W. Kogler, M. Tietz and W. J. Auhorn, in *Ullmann's Encyclopedia of Industrial Chemistry*, 2012.

TOC description: one sentence of text, maximum 20 words, highlighting the novelty of the work:

"A fluorescent macromolecular chemosensor, built from readily available components, performs chemical fingerprinting of carboxylate anions on low-cost, disposable paper supports."

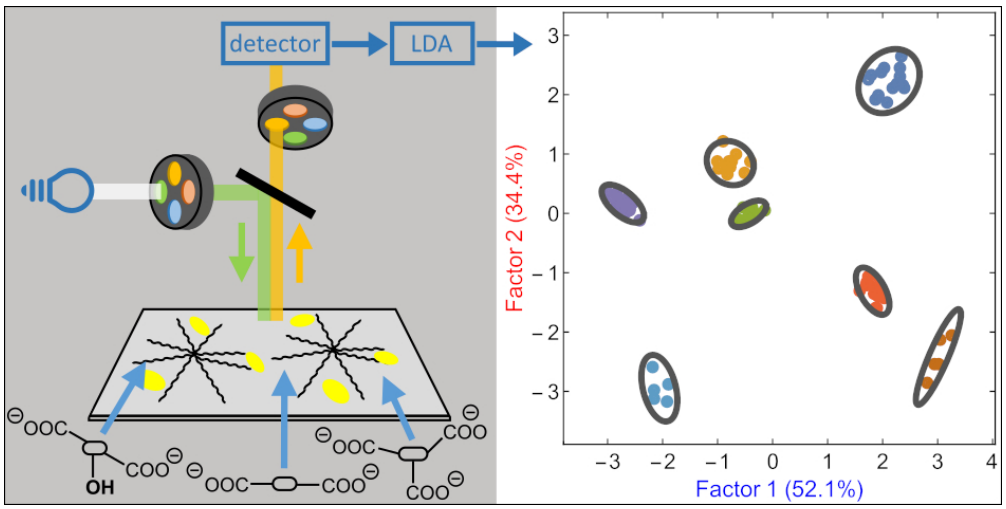
detector
LDA
Factor 2 (34.4%)
Factor 1 (52.1%)
3
2
1
0
−1
−2
−3
−3
−2
−1
0
1
2
3
4
OH
COO
OOC